# 8-Tbps (20 × 400 Gbps) Unrepeated Transmission over 80 km with 2-THz PPLN-Based Phase-Sensitive Amplification Using Precise Chromatic Dispersion Pre-Compensation

Shimpei Shimizu(1), Takayuki Kobayashi(1), Takushi Kazama(1,2), Takeshi Umeki(1,2), Masanori Nakamura(1), Koji Enbutsu(2), Ryoichi Kasahara(2), Yutaka Miyamoto(1)

(1) NTT Network Innovation Laboratories, NTT Corporation, 1-1 Hikarinooka, Yokosuka, Kanagawa, Japan, shimpei.shimizu.ge@hco.ntt.co.jp

(2) NTT Device Technology Laboratories, NTT Corporation, 3-1 Morinosato, Wakamiya, Atsugi, Kanagawa, Japan

**Abstract** *We demonstrate an 80-km unrepeated transmission of a 20-ch. 96-Gbaud PS-64QAM WDM signal with 100-GHz spacing using a periodically poled $LiNbO_3$-based phase-sensitive amplifier. We achieve widest-band simultaneous phase-sensitive amplification over 2 THz (4 THz including an idler band) by precise chromatic dispersion pre-compensation.*

## Introduction

Optical transport networks based on digital-coherent technology and wavelength division multiplexing (WDM) supported by erbium-doped fibre amplifiers (EDFAs) are widely deployed. The demand for high-speed optical channels has increased with the exponential surge in communication traffic. 1-Tbps channels have been achieved by using symbol rates higher than 100 Gbaud and higher-order modulation formats[1]. However, such high-speed channels require a higher optical signal-to-noise ratio (OSNR), and thus, their operation ranges with respect to transmission power and distance are narrow. Therefore, it is important to reduce the noise of optical amplifiers to expand the operation range and to achieve higher-speed optical channels.

Phase-sensitive amplifiers (PSAs) by means of optical parametric amplification (OPA) enable high OSNR by low-noise amplification outperforming EDFAs[2]. OPA is an optical nonlinear process in highly nonlinear media such as periodically poled $LiNbO_3$ (PPLN) waveguides and highly nonlinear fibres. In particular, PPLN-based OPA modules can achieve both high gain and wideband amplification, and their potential as optical repeaters exceeding 10 THz has been demonstrated with a 120-Gbaud WDM signal[3]. The phase-sensitive amplification of QAM signals has been demonstrated using frequency non-degenerate PSA (ND-PSA)[4]–[6]. However, one of the most important problems for ND-PSA is the effect of chromatic dispersion (CD) on the signal and idler lights. ND-PSAs require CD compensation because it is necessary to make the relative phase between the signal and idler lights uniform in the frequency domain. The wider the amplification bandwidth, the more precise the requirement of CD compensation accuracy[7]. Therefore, the maximum bandwidth of simultaneous amplification of a fibre-transmitted WDM signal was 1.6 THz[4]. In addition, symbol rates in transmission experiments using PSAs were typical rates of less than 40 Gbaud.

In this paper, we perform an 80-km unrepeated transmission with 20-ch. 96-Gbaud probabilistically shaped 64QAM (PS-64QAM) signals using PPLN-based OPA modules as the widest-band simultaneous phase-sensitive amplification. The WDM signal is implemented with 100-GHz spacing over 2 THz, and the total capacity is 8 Tbps. We apply a precise CD estimation and compensation method[7] for wideband phase-sensitive amplification. An ND-PSA is used as a pre-amplifier, and its noise performance are compared with an EDFA.

## Experimental setup

Figure 1 shows the experimental setup for an 80-km unrepeated transmission using a PPLN-based ND-PSA with a 20-ch. WDM signal. The modulation format was Nyquist-pulse-shaped 96-Gbaud single-polarised (SP-) PS-64QAM with the same entropy per polarisation component as a reference[1]. We configured a copier-PSA scheme[4],[5], in which idler lights (phase conjugation of signals) are generated by the OPA as an optical phase conjugator (OPC) at the transmitter side. The phase-matching frequency of our PPLN waveguides was 194.0 THz. We utilised a two-stage configuration consisting of a cascade of two PPLNs for second-harmonic generation (SHG) as the pump light conversion and OPA[8]. The frequency stabilisation of the pump light for phase-sensitive amplification was performed by an optical injection locking (OIL) using a co-transmitted pilot light. WDM channels

978-0-7381-4679-9/21/$31.00 ©2021 IEEE

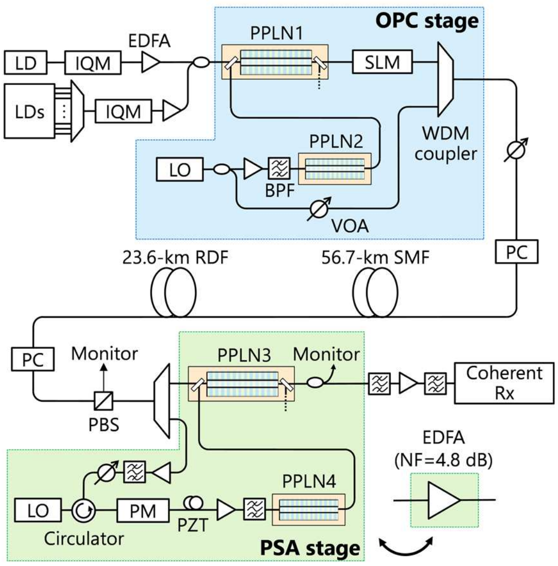


**Fig. 1:** Experimental setup. LD: laser diode, IQM: I/Q modulator, VOA: variable optical attenuator, PC: polarisation controller, PBS: polarisation beam splitter, PZT: piezoelectric transducer-based fibre stretcher, BPF: band-pass filter, LO: local oscillator, PM: phase modulator.

were densely allocated in a 100-GHz grid from 191.95 to 193.95 THz. The gain of the OPA in the OPC stage was 12 dB. The local oscillator (LO) driven at 194.0 THz was divided using a 3-dB coupler as the pump light in the OPC stage and the pilot light for the OIL. The pump light was amplified by a 1.55-μm-band EDFA and then converted to a second harmonic light by the SHG. The pilot light was inserted into the WDM signals after the idler generation with a power of −18.0 dBm at the input of the transmission link. The WDM signals with the pilot light and idlers were input to the PSA stage via an 80.3-km CD-managed transmission link consisting of a 56.7-km single-mode fibre (SMF) and a 23.6-km reverse-dispersion fibre (RDF). In addition, as described in the next section, the slight residual CD was precisely pre-compensated with a spatial light modulator (SLM). The SLM could modulate a phase of input light in the frequency domain with a 1-GHz resolution. The propagation loss of this link was 19.3 dB at 194.0 THz. The averaged fibre-input power was set to −14.3 dBm/ch. Before pre-amplification, only the TM polarisation component of the signal light was extracted with the polarisation controllers (PCs) at both ends of the transmission link and a polarisation beam splitter (PBS) because PPLN waveguides have polarisation sensitivity. The PCs were adjusted so that the optical power in the monitor port of the PBS was the lowest. In the PSA stage, the phase-sensitive amplification was performed using a frequency-stabilised LO with the OIL. The relative phase drift between the signal and pump lights was compensated by a piezoelectric-transducer-based phase-locking loop (PZT-PLL). A phase modulator (PM) was used for modulating a dither signal for the PZT-PLL. The PZT-PLL monitored a 10% tapped channel at 193.5 THz as the locking frequency. The gain of the PSA stage was 20 dB. The pre-amplified WDM signals were received by a coherent receiver and demodulated in offline digital signal processing on the basis of 8×1 MIMO equaliser[1]. The signal qualities were evaluated by calculating their normalised generalised mutual information (NGMI) and SNR on the basis of the variance of the signal from desired symbols. We assumed that the forward error correction (FEC) threshold of the NGMI was 0.857 with a net data rate of 404.72 Gbps/ch.[1]. To evaluate the noise performance of the PSA, an experiment in which the PSA stage was replaced with an EDFA (typical NF = 4.8 dB) operating at the same gain of the PSA was conducted.

### Precise CD pre-compensation

Phase-sensitive amplification requires a CD compensation because relative phase between the pump light and all signal-idler pairs need to synchronise. The residual CD causes gain ripple and passband narrowing[9]. The wider amplification bandwidth, the more precise CD compensation is required. In addition, higher-symbol-rate signals have a greater degradation on the signal quality even with the same passband narrowing. We applied the residual CD estimation and compensation method using a gain characteristic of PSA[7] for realizing wideband amplification of a 100-Gbaud-class WDM signal. Figure 2 shows the spectrum of a 20-ch. WDM signal measured by an optical spectrum analyser after the 80-km transmission and phase-sensitive amplification. The spectrum

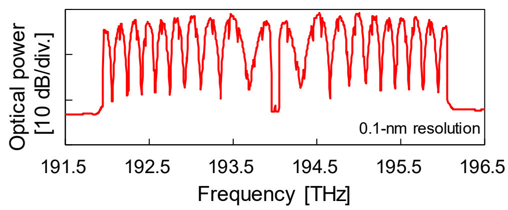


**Fig. 2:** Spectrum of WDM signal after phase-sensitive amplification without CD pre-compensation.

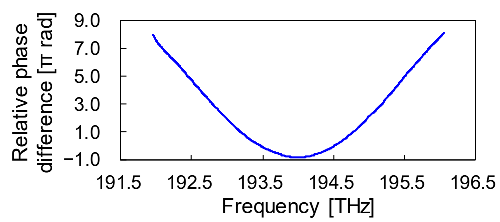


**Fig. 3:** Calculated relative phase difference from locking frequency due to residual CD.

suffered from gain ripple due to the slight residual CD in our CD-managed link. The amount of residual local CD can be estimated from the frequencies of (de-)amplification points in this spectrum and the locking frequency of the PZT-PLL. The CD estimated from amplification points is expressed as

$$D = \frac{f_0^2}{c\left(B_m^{\;2} - \Delta f^2\right)} m, \qquad (1)$$

and that estimated from de-amplification points is expressed as

$$D = \frac{f_0^2}{2c\left(B_m^{\;2} - \Delta f^2\right)} m, \qquad (2)$$

where, $f_0$ is the centre frequency of the amplification band, $c$ is the speed of light, $B_m$ is the bandwidth between $f_0$ and the $m$th (de-)amplification point, and $\Delta f$ is the bandwidth between $f_0$ and the locking frequency. Figure 3 shows the relative phase difference from the locking frequency calculated by the estimated CD. The averaged residual local CD was 0.334 ps/nm. We compensated for this relative phase difference in the WDM signal using the SLM.

## 80-km transmission of 20-ch. 96-Gbaud SP-PS-64QAM signals

Figure 4 shows the pre-amplified spectra in the PSA and EDFA-only cases. The input spectrum was measured at the PBS input. The wideband phase-sensitive amplification over 4 THz including the idler band without gain ripple was performed due to the precise CD compensation. The differences in noise floor between the PSA and EDFA-only cases were 8.1 dB at 191.50 THz and 8.8 dB at 193.97 THz. Considering the EDFA output unpolarised amplified spontaneous emission (ASE) light, OSNR improvements were estimated to be about 5.1–5.8 dB depending on the frequency. Figure 5 shows the NGMIs and constellation diagrams of the received 20 WDM channels. In the EDFA-only case, NGMIs did not exceed the FEC threshold for a net data rate of 404.72 Gbps due to the low-input power.

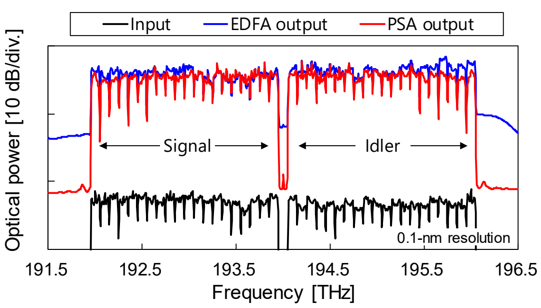


**Fig. 4:** WDM spectra after pre-amplifying by PSA or EDFA.

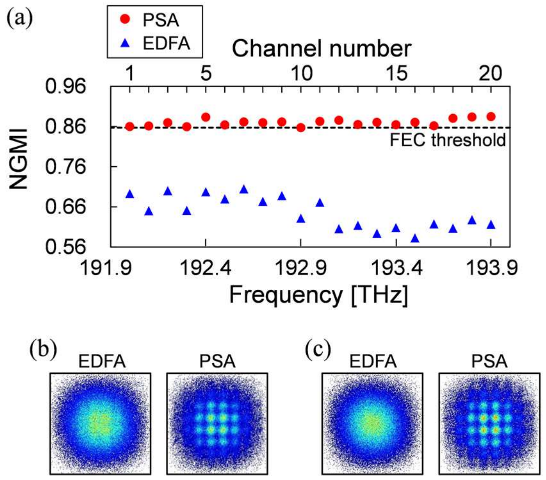


**Fig. 5:** Received signal characteristics. (a) NGMIs of 20-ch. 96-Gbaud SP-PS-64QAM signals. Constellation diagrams of (b) ch.1 and (c) ch.20.

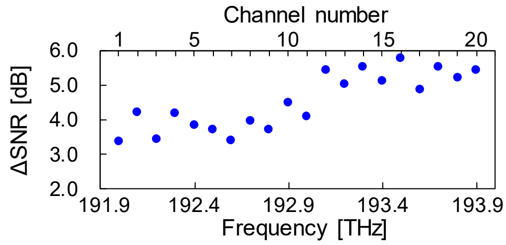


**Fig. 6:** ΔSNR characteristic indicates SNR improvement amount by PSA in each channel.

However, NGMIs of all channels exceeded the threshold in the PSA case thanks to the OSNR improvements. Figure 6 shows the ΔSNR characteristics, which are the differences in SNR between the PSA and EDFA-only cases. The highest ΔSNR was 5.7 dB at ch.16 (193.5 THz). As ch.16 was the locking point of the PZT-PLL, the stable phase-sensitive amplification was performed. ΔSNR tended to decrease as the distance from the centre frequency increased due to a mismatch of the polarisation states between the signal and idler lights[10]. We attempted to extract only the TM polarisation with PCs, but it was difficult to perfectly match the random polarisation rotation in the transmission fibres between the distant signals and idlers.

## Conclusion

We demonstrated an unrepeated transmission of 20-ch. 96-Gbaud SP-PS-64QAM signals using PPLN-based OPA modules as the widest-band simultaneous phase-sensitive amplification. Low-noise amplification outperforming an EDFA was shown over a 2-THz signal band (4 THz including the idler band) due to precise CD compensation. The 80-km transmission with a net data rate of 8 Tbps (20 × 400 Gbps) was successful under a condition that could not be achieved by using an EDFA-only pre-amplifier.

## References


[1] T. Kobayashi, M. Nakamura, F. Hamaoka, M. Nagatani, H. Wakita, H. Yamazaki, T. Umeki, H. Nosaka, and Y. Miyamoto, “35-Tb/s C-band Transmission over 800 km Employing 1-Tb/s PS-64QAM Signals enhanced by Complex 8 × 2 MIMO Equalizer,” in *Proc. Opt. Fiber Commun. Conf. (OFC)*, Th4B.2, Mar. 2020.

[2] W. Imajuku, A. Takada, and Y. Yamabayashi, “Low-noise amplification under the 3-dB noise figure in a high gain phase-sensitive fiber amplifier,” *Electron. Lett.*, vol. 35, no. 22, pp. 1954–1955, Oct. 1999.

[3] T. Kobayashi, S. Shimizu, M. Nakamura, T. Umeki, T. Kazama, R. Kasahara, F. Hamaoka, M. Nagatani, H. Yamazaki, H. Nosaka, and Y. Miyamoto, “Wide-Band Inline-Amplified WDM Transmission Using PPLN-Based Optical Parametric Amplifier”, *IEEE J. Lightwave Technol.*, vol. 39, no. 3, pp. 787–794, Feb. 2021.

[4] T. Umeki, T. Kazama, T. Kobayashi, S. Takasaka, Y. Okamura, K. Enbutsu, O. Tadanaga, H. Takenouchi, R. Sugizaki, A. Takada, R. Kasahara, and Y. Miyamoto, “Polarization-diversity In-line Phase Sensitive Amplifier for Simultaneous Amplification of Fiber-transmitted WDM PDM-16QAM Signals,” in *Proc. Opt. Fiber Commun. Conf. (OFC)*, M3E.4, Mar. 2018.

[5] Z. Tong, C. Lundstrom, P. A. Andrekson, C. J. McKinstrie, D. J. Blessing, E. Tipsuwannakul, B. J. Puttnam, H. Toda, and L. Gruner-Nielsen, “Towards ultrasensitive optical links enabled by low-noise phase-sensitive amplifiers,” *Nat. Photonics*, vol. 5, no. 7, pp. 430–436, July 2011.

[6] Y. Akasaka, Y. Cao, S. Takasaka, K. Yamauchi, K. Maeda, H. Song, R. Sugizaki, A. E. Willner, and T. Ikeushi, “WDM Amplification of One Pump HNLF Based Phase Sensitive Amplifier with Static Pump Phase Tuning,” in *Proc. Opt. Fiber Commun. Conf. (OFC)*, W4F.5, Mar. 2019.

[7] S. Shimizu, T. Kazama, T. Kobayashi, T. Umeki, K. Enbutsu, R. Kasahara, and Y. Miyamoto, “Accurate Estimation of Chromatic Dispersion for Non-Degenerate Phase-Sensitive Amplification,” *IEEE J. Lightwave Technol.*, vol. 39, no. 1, pp. 24–32, Jan. 2021.

[8] T. Kazama, T. Umeki, M. Abe, K. Enbutsu, Y. Miyamoto, and H. Takenouchi, “Low-Parametric-Crosstalk Phase-Sensitive Amplifier for Guard-Band-Less DWDM Signal Using PPLN Waveguides,” *IEEE J. Lightwave Technol.*, vol. 35, no. 4, pp. 755–761, Aug. 2016.

[9] S. Shimizu, T. Kazama, T. Kobayashi, T. Umeki, K. Enbutsu, R. Kasahara, and Y. Miyamoto, “Gain Ripple and Passband Narrowing due to Residual Chromatic Dispersion in Non-Degenerate Phase-Sensitive Amplifiers,” in *Proc. Opt. Fiber Commun. Conf. (OFC)*, M1I.3, Mar. 2020.

[10] A. L.-Riesgo, P. A. Andrekson, and M. Karlsson, “Polarization-Independent Phase-Sensitive Amplification, “ *IEEE J. Lightwave Technol.*, vol. 34, no. 13, pp. 3171–3180, July 2016.